The Mixing of Solids in Slugging Gas Fluidized Beds

Measurements have been made of axial solids mixing in fluidized beds of 0.05, 0.1, and 0.22 m diameter with a variety of materials at atmospheric pressure. Round nosed slugs, raining slugs, and turbulent bubbling have been investigated. Raining slugs occur with coarser materials. With cracking catalyst round nosed slugs form readily in the smaller diameter beds, but in the largest bed, breakdown to the turbulent state was normal. A model has been developed to predict the axial solids mixing in a slugging fluidized bed containing round nosed slugs. The model supposes that each slug is followed by a well-mixed wake and a piston flow region. The model predicts well the scale effect noted by W. G. May. Axial mixing is fast for round nosed slugs, falls for turbulent bubbling, and is low for raining slugs.

WILLIAM J. THIEL
and
OWEN E. POTTER
Department of Chemical Engineering
Monash University
Clayton 3168, Victoria, Australia

SCOPE

W. G. May drew attention to a marked scale effect in the mixing of solids in fluidized beds. No explanation has been forthcoming. Davidson has pointed out that in many cases the fluidized beds experimented with have been slugging; that is, the bubbles have an equivalent spherical diameter approaching or exceeding that of the vessel. In this paper, a model is presented, based on the slugging fluidized bed, which accounts for the scale effect and gives a reasonable prediction of the axial dispersion coefficients.

CONCLUSIONS AND SIGNIFICANCE

Much interest attaches to fluidization processes at this time, arising from the study of coal liquefaction and gasification by various processes and from environmental considerations such as have influenced the development of fluidized combustion. Insofar as initial experimentation and pilot plants are concerned with relatively small diameter vessels, the slugging fluidized bed needs to be thoroughly understood. Slugging is not a unique state and may exist in different forms. Round nosed slugs are regular in behavior and have a predictable rise velocity. Owing no doubt to particle to particle forces, assymetric slugs may rise along the wall, with predictable velocities, or square nosed (raining) slugs may form. In the latter case, gas passes through the bed partly by slug flow and partly by packed-bed flow when solids lock onto the wall. In this paper, it is shown that a model which assumes that a wake of well-mixed solids rises behind the round nosed slug is sufficient to provide a reasonable prediction of the dispersion coefficient. It is also shown that with coarser solids square nosed (raining) slugs form and the axial dispersion coefficient is greatly reduced. For fine materials such as cracking catalyst, which form round nosed slugs, it is found that these slugs may break down to form small bubbles in what Davidson and co-workers have called the turbulent state. The dispersion coefficient is high in such case but less than with round nosed slugs.

The model supposes that the interslug space between round nosed slugs can be divided into a perfectly mixed and piston flow regions. Parameter a is the fraction of the total interslug space which is perfectly mixed. The model fits the authors' experimental results for values of a between 0.5 and 0.85. It is also shown to fit the data in the literature and to correctly predict the scaling effect for varying bed diameter for a value of $a = 0.7$.

The significance is that a model has been given which accounts for dispersion and the scale effect with materials such as cracking catalyst, and that material properties are of great significance in slugging fluidized beds and changes in particle size can lead to a very different state of fluidization, solids mixing, and gas mixing.

William J. Thiel is at Victorian College of Pharmacy, Melbourne, Australia.

0001-1541-78-1138-0561-$01.15.

In a gas fluidized bed of high aspect ratio, rapid bubble coalescence near the distributor leads to the formation of large gas bubbles or slugs. The rise velocity of the gas slugs is limited by the proximity of the walls of the containing vessel. Two main gas flow regimes can be observed in slugging fluidized beds (Stewart and Davidson, 1967). The first regime, the smoothly slugging bed, contains round nosed slugs, similar to those which form in a liquid, and the particulate phase flows down past the rising slug in an annular region on the wall. The second regime, the raining slug bed, is so called because the solids rain through the gas slug from a flat ceiling above. The raining slug is square nosed and exists across the complete bed diameter.

In recent years, considerable interest has been shown in slugging beds, due mainly to two factors. Firstly, the realization that most of the laboratory data in the literature have been obtained in small diameter beds, where bubble size was such that the rise velocity was limited by the bed wall. In fact, many smaller industrial reactors are now thought to operate close to or under slugging conditions. Secondly, the slug flow regime is easier to characterize than the freely bubbling bed, as slugs are evenly spaced, have a characteristic rise velocity, and coalesce little except near the distributor. This makes the analysis of the slugging bed less complex and the results easier to interpret than for the freely bubbling bed, where bubble size and rise velocity change continuously.

For certain industrial applications, the slugging bed has positive advantages. The axial mixing of solids in the raining slug bed is low, which leads to better conversions in the catalytic oxidation of naphthalene to phthalic anhydride and anthracene to anthraquinone than is achieved in a normal fluidized bed (Gelperin et al., 1970).

A number of studies of axial solids mixing in fluidized beds have been made, and it is shown later that most of the beds were operating in slug flow. These studies report only mixing data, and parameters such as slug rise velocity and slug spacing do not appear.

The aim of the work reported here was to develop a model for the mixing of solids in a smoothly slugging fluidized bed and to test this model with experimental data from three different diameter slugging beds, which had been carefully characterized. The largest bed was of small industrial size, being 0.218 m diameter and 6.9 m high.

PREVIOUS WORK

The Onset of Slug Flow

The rise velocity of a gas bubble is markedly influenced by the proximity of the bed wall if $D_e/D \geqq 1/3$ (Matsen and Tarmy, 1970), and under these conditions the rise velocity of an isolated slug (U_{SD}) is given by

$$U_{SD} = 0.35(gD)^{1/2} \tag{1}$$

The rise velocity of continuously generated gas slugs in a fluidized bed, where coalescence is minimal, is given by

$$U_{SA} = (U - U_{mf}) + 0.35(gD)^{1/2} \tag{2}$$

Using this value for rise velocity and an interslug spacing (T) of two tube diameters, Stewart and Davidson (1967) develop the following criterion for the onset of the smoothly slugging regime in a bed:

$$\frac{U - U_{mf}}{U_{SD}} = \frac{U - U_{mf}}{0.35(gD)^{1/2}} = 0.2 \tag{3}$$

TABLE 1. INTERSLUG SPACING T IN VARIOUS DIAMETER SMOOTHLY SLUGGING BEDS

Bed diameter (m)	Range of values of T observed	Reference
0.051	5-8	Thiel and Potter (1977)
0.102	2-5	Kehoe and Davidson (1970)
0.102	3-5	Thiel and Potter (1977)
0.140	2.4	Matsen and Tarmy (1970)
0.218	2-3	Thiel and Potter (1977)
0.460	1-2	Hovmand and Davidson (1968)

Slug Properties in Smoothly Slugging Beds

The rise velocity of continuously generated slugs is described by Equation (2). Matsen and Tarmy (1970) give the following expression for slug length:

$$L_S = \frac{TD(U - U_{mf})}{0.35(gD)^{1/2}} \tag{4}$$

A correction may be made to account for the slug shape (Kehoe and Davidson, 1970); this gives the slug length as

$$\frac{L_S}{D} - 0.495\left(\frac{L_S}{D}\right)^{1/2}\left(1 + \frac{U - U_{mf}}{0.35(gD)^{1/2}}\right) + 0.061 - (T - 0.061)\left(\frac{U - U_{mf}}{0.35(gD)^{1/2}}\right) = 0 \tag{5}$$

which can be approximated by

$$L_S = JD(U - U_{mf})/0.35(gD)^{1/2} \tag{6}$$

The values of J are

T	1	2	3	4	5	6	7
J	2.44	3.83	5.41	6.41	7.63	8.84	10.00

T is dimensionless and equals interslug spacing divided by bed diameter. Experimental values of T measured by a number of workers are shown in Table 1.

The frequency of slugs in a smoothly slugging bed is given by Matsen and Tarmy (1970):

$$f = \frac{0.35g^{1/2}}{TD^{1/2}} \tag{7}$$

Gas Flow Regimes in Slug Flow

As already discussed, two main slug flow regimes have been reported. The smoothly slugging regime occurs in beds of diameter greater than 0.05 m with materials which fluidize easily. Hovmand and Davidson (1971) consider the raining slug regime to be a breakdown of proper fluidization which occurs in beds of diameter less than 0.05 m.

More recently, the present authors have shown (Thiel and Potter, 1977) that this observation is in need of qualification. The raining regime can occur in high aspect ratio beds of diameter up to 0.22 m. It was shown that the angles of internal friction of the particulate solid and bed diameter are significant in determining which slug flow regime will form in a high aspect ratio bed. A mechanism is proposed to explain the formation of a raining bed (Thiel and Potter, 1977).

TABLE 2. GAS FLOW RATE FOR THE ONSET OF SLUG FLOW

Author	Bed diameter (m)	Solid	Bed height (m)	U-U_{mf} for onset slug flow from Equation (3) (m/s)	Range U-U_{mf} used in work (m/s)
Miyauchi et al. (1968)	0.079	FCC	3.0	0.062	0.2-0.4
May (1959)	0.050	FCC	9.8	0.054	0.244
May (1959)	0.380	FCC	9.8	0.140	0.244
May (1959)	1.520	FCC	9.8	0.275	0.244
Lewis et al. (1961-62)	0.075	FCC	Approximate 2.3	0.060	0.06-0.30
Shrikhande (1955)	0.074	Glass microspheres	1.9	0.060	0.04-0.89
de Groot (1967)	0.100	Silica	3.3	0.084	0.1-0.2
de Groot (1967)	0.300	Silica	3.2	0.135	0.1-0.2
de Groot (1967)	0.600	Silica	2.3	0.185	0.1-0.2
de Groot (1967)	1.500	Silica	4.7	0.284	0.1-0.2

Kehoe and Davidson (1970) report that the smoothly slugging regime breaks down to form a turbulent regime, with fine powders, at gas velocities of approximately three times the terminal falling velocity of the particles. Thiel and Potter (1977) observed the turbulent regime in a larger diameter bed (0.22 m) at a much lower superficial gas velocity.

Solids Mixing

A number of authors report the results of solids mixing experiments in the form of an axial solids diffusivity. Two methods have been used to investigate the solids mixing, steady state heat transfer (Miyauchi et al., 1968; Shrikhande, 1955; Lewis et al., 1961-62) and radioactive tracer studies (May, 1959; de Groot, 1967). If the criterion for the onset of slug flow [Equation (3)] is applied to these studies, it is shown in Table 2 that nearly all the work was conducted in beds in slug flow.

Miyauchi et al. (1968) and Lewis et al. (1961-62) relate the effective axial thermal conductivity of the bed to an effective axial solids diffusivity (E_S) by assuming that solids in the bed are in thermal equilibrium across a section and by justifiably ignoring the contribution of the gas to thermal transport:

$$E_S = \frac{\kappa}{\rho_S C_S \epsilon_S} \tag{8}$$

If ϵ_S is the fraction of the total bed which is solids, an apparent axial solids diffusivity $\overline{E}_S$ can also be defined Miyauchi et al. (1968):

$$\overline{E}_S = \epsilon_S E_S = \frac{\kappa}{\rho_S C_S} \tag{9}$$

May (1959) and de Groot (1967) fitted their results for the unsteady state mixing of radioactive tracer particles to a one-dimensional diffusion model of the form

$$E_S \left(\frac{\partial^2 C}{\partial x^2}\right) = \frac{\partial C}{\partial t} \tag{10}$$

to predict the axial solids diffusivity E_S. In none of these investigations have the fluidized beds been characterized in terms of slug rise velocity, slug frequency, or slug spacing. The most noticeable feature of all the results is the very high degree of scatter of the solids mixing results for different solids in different diameter beds.

MODEL FOR SOLIDS MIXING IN A SMOOTHLY SLUGGING BED

As a first assumption, the region between regularly spaced gas slugs in a smoothly slugging bed is assumed to consist entirely of a perfectly mixed wake, which is responsible for the axial transport and mixing of solids. The basis for this assumption is that bubble wakes are known to be the main mechanism of solids mixing in a freely bubbling bed (Woollard and Potter, 1968; Rowe et al., 1965), and the mechanism of coalescence of slugs is thought to be the same as for gas bubbles (Harrison and Leung, 1962). Thus, in a high aspect ratio bed, where slug coalescence is minimal, the region between slugs will be mainly filled by a well-mixed wake.

The solids mixing in the dense phase between continuously generated gas slugs is therefore, in the first instances, represented as that of a series of perfectly mixed cells, solids feeding downwards from cell to cell as the slugs rise. The top cell empties past the uppermost slug until the slug reaches the bed surface, at which time the top cell is just empty. The cell below then becomes the top cell. This process is illustrated in Figure 1.

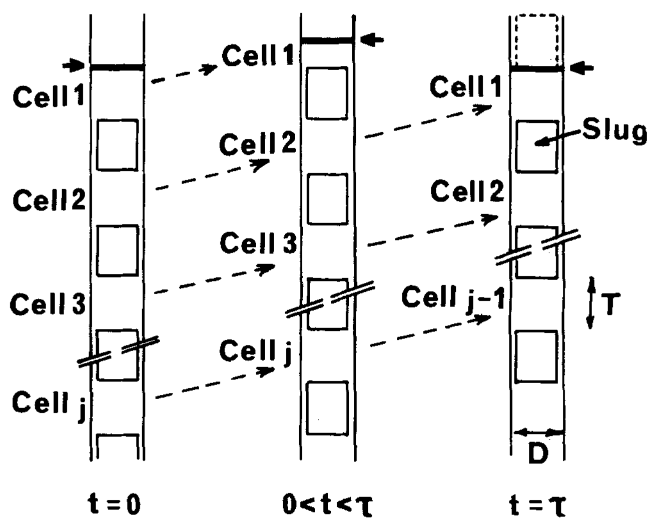

Fig. 1. Schematic illustrating the cyclic process of the slugging fluidized bed. The cells are renumbered at $t = \tau$ consequent on the disappearance of cell 1. The slug rise velocity relative to the bed surface (marked ←) is U_{SD}.

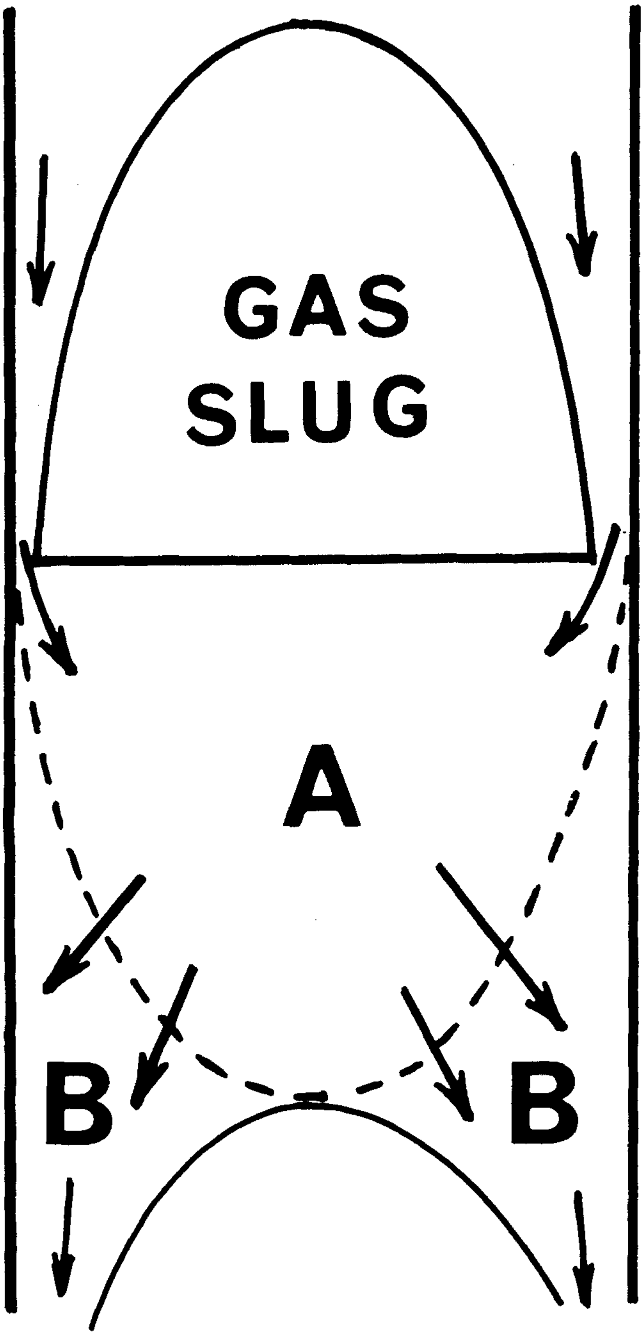

Fig. 2. The parabolic wake region behind a gas slug. A—parabolic wake, solids well mixed. B—solids in plug flow. Arrows indicate the flow of solids.

Consider a theoretical experiment, similar to those which have been performed, in which heat is continuously added to the bottom of a slugging bed and continuously removed from the top cell. The top cell is assumed to have a constant temperature due to heat removal, which is used as a reference temperature for the heat balance equations and arbitrarily set equal to zero. Solids convection is assumed to be the only mechanism of heat transfer.

A time constant τ is defined for each solids mixing cell, which is the cell volume (V) divided by the volumetric flow rate (v) between cells. Referring to Figure 1 which shows the bed surface just as the top slug bursts, we get

$$V = \left(\frac{\pi D^2}{4}\right) TD \tag{11}$$

The volumetric flow rate between cells is the volume of the cell divided by the time taken for the next slug in the bed to reach the surface:

$$v = \left(\frac{\pi D^2}{4}\right) TD \Bigg/ \frac{TD}{U_{SD}} \tag{12}$$

The time constant τ is given by

$$\tau = \frac{V}{v} = \frac{TD}{U_{SD}} \tag{13}$$

The series of cells can now be treated mathematically exactly the same as a series of perfectly mixed tanks. If we number the cells from the top, cell 1 has a constant temperature, due to heat removal.

The temperature in cell j is θ_j; the output from cell j has a temperature of θ_j and an input temperature of θ_{j-1}. A particular cell j exists for a time interval τ at which time the top cell disappears as the top gas slug reaches the surface. The cells are then renumbered, and cell j becomes cell $j - 1$. The voidage in the dense phase is assumed to be ϵ_{mf}, and the solids density is ρ_S. During the time interval τ, the cell temperature variations with respect to time are described by a set of heat balance equations which are detailed in the Appendix.

The average temperature difference between cells determined from heat balance equations is 0.73 θ_{20} (θ_{20} is the temperature of cell 2 at time $t = 0$). When cell 2 becomes cell 1, heat is removed. At every τ an amount of heat is removed from the top cell causing a temperature change from $\theta_{2\tau}$ to zero. The heat removed in a time τ is

$$TD\left(\frac{\pi D^2}{4}\right) C_S\rho_S(1 - \epsilon_{mf})\theta_{2\tau} = TD\left(\frac{\pi D^2}{4}\right) C_S\rho_S(1 - \epsilon_{mf})\frac{\theta_{20}}{e} \tag{14}$$

Therefore, the heat flux is

$$U_{SD}C_S\rho_S(1 - \epsilon_{mf})\frac{\theta_{20}}{e} \tag{15}$$

The axial temperature gradient is

$$\frac{0.73\,\theta_{20}}{L_S + TD} \tag{16}$$

where the slug length L_S is given by Equation (4). From the heat flux and axial temperature gradient, the effective axial thermal conductivity is

$$\kappa = \frac{(1 - \epsilon_{mf})\rho_S C_S TD[(U - U_{mf}) + 0.35(gD)^{1/2}]}{0.73e} \tag{17}$$

If we use Equation (9), the effective axial solids diffusivity is

$$\overline{E}_S = \frac{(1 - \epsilon_{mf})TD[(U - U_{mf}) + 0.35(gD)^{1/2}]}{0.73e} \tag{18}$$

Equation (18) is not satisfactory for low gas flow rates as $U - U_{mf} \rightarrow 0$. Values of $\overline{E}_S$ calculated from Equation (18) are tabulated by Thiel (1972). Comparison of Equation (18) with experimental values of effective axial solids diffusivity, measured in beds of fluid cracking catalyst, indicate that the model overestimates the solids mixing by a factor of approximately two.

The assumption was made that the entire interslug space was filled with a perfectly mixed wake. If the well-mixed wake region only occupies a volume of parabolic cross section, as shown in Figure 2, then the wake region occupies half the interslug space. The mixing behind a gas slug in this case can be represented as a perfectly mixed cell of volume $V/2$ in series with a plug flow cell of volume $V/2$. A similar method of analysis, to that already discussed, is then used (Thiel, 1972). This model predicts a value of $\overline{E}_S$ equal to one quarter of that predicted by Equation (18):

$$\overline{E}_S = \frac{1}{4}\frac{(1-\epsilon_{mf})TD[U - U_{mf} + 0.35(gD)^{1/2}]}{2} \tag{19}$$

Equation (18) and the result just given can be proved independently by considering the correspondence between the dispersion model and the tanks in series model (Levenspiel, 1962). Equating the variance of the C curve for each model, we get

$$\text{Variance} = \frac{1}{j} = \frac{2D_S}{uL} - 2\left(\frac{D_S^2}{uL}\right)\left(1 - e^{\frac{-uL}{D_S}}\right) \tag{20}$$

If D_S/uL is small, this equation approximates to

$$\frac{1}{j} = \frac{2D_S}{uL} \tag{21}$$

Now $L = j\zeta$, where ζ is the length of a mixing cell. For a slugging bed, $\zeta = TD$

$$\frac{1}{j} = \frac{2D_S}{ujTD} \tag{22}$$

$$D_S = \frac{uTD}{2} = \frac{TDU_{SA}}{2} \tag{23}$$

where U_{SA} is given by Equation (2):

$$\overline{E}_S = (1-\epsilon_{mf})D_S = \frac{(1-\epsilon_{mf})TDU_{SA}}{2} \tag{24}$$

which is the same as Equation (18).

Using the method of Levenspiel (1962), Thiel (1972) showed that the variance of the C curve for a series of mixing cells connected by plug flow sections is a^2/j, where a is the fraction of the interslug volume which is perfectly mixed. Again, matching the C curve for a series of perfectly mixed and plug flow cells to that of the dispersion model, we get

$$\text{Variance} = \frac{a^2}{j} = \frac{2D_S}{uL} \tag{25}$$

$$L = jTD \tag{26}$$

$$D_S = a^2\frac{TDU_{SA}}{2} \tag{27}$$

and

$$\overline{E}_S = \frac{a^2(1-\epsilon_{mf})TD[U - U_{mf} + 0.35(gD)^{1/2}]}{2} \tag{28}$$

which is a general form of Equation (19) for any value of a. Values of $\overline{E}_S$ calculated from Equation (28) for various values of the parameter a are shown in Figures 5, 6, and 7.

During the derivation of Equation (28), the slug length was predicted using Equation (4). A correction for slug shape can be introduced using Equation (6) which gives the axial solids diffusivity in a series of perfectly mixed and plug flow cells as

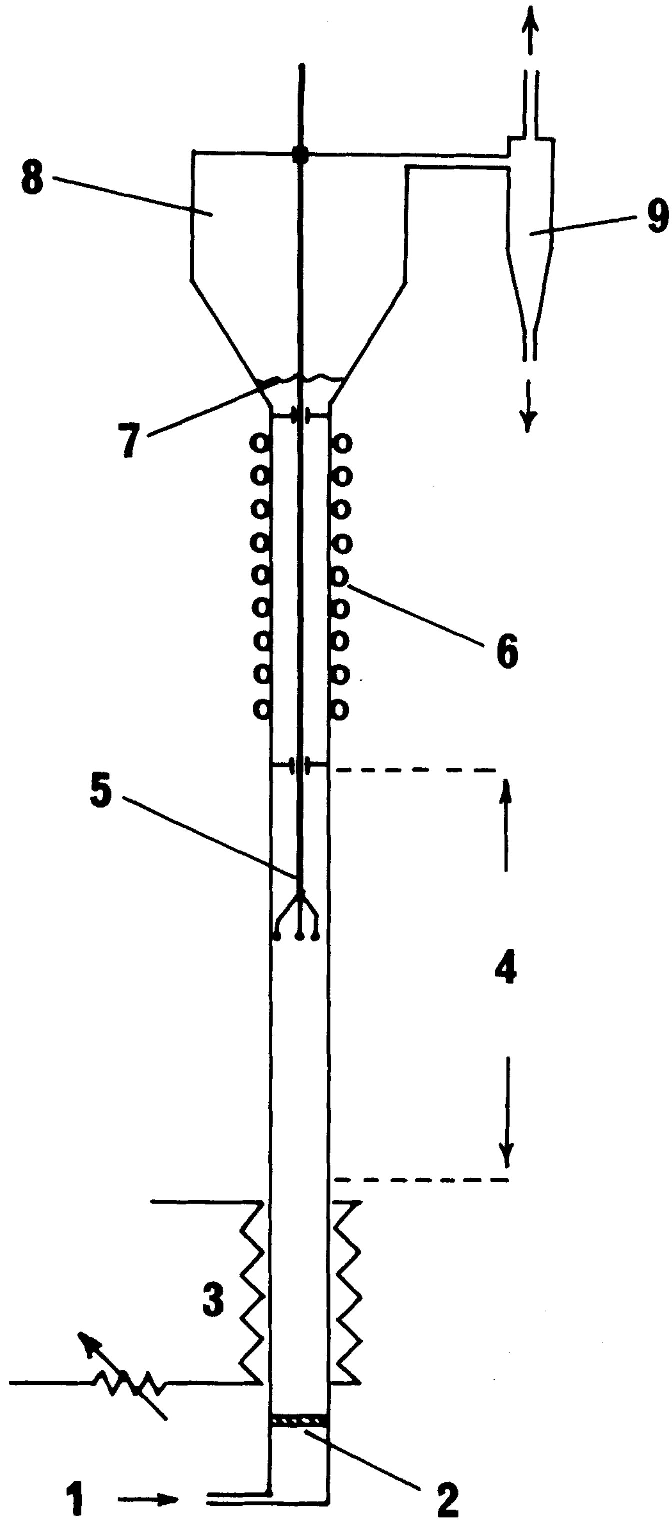

Fig. 3. Arrangement of the apparatus: 1 air inlet, 2 distributor, 3 electric heaters, 4 experimental section, 5 thermocouple probe, 6 cooling coils, 7 bed surface, 8 disengaging section, 9 cyclone separator.

$$\overline{E}_S = \frac{a^2TD(1-\epsilon_{mf})\left(\frac{J}{T}\right)[U - U_{mf} + 0.35(gD)^{1/2}]}{2} \tag{29}$$

EXPERIMENTAL WORK

Apparatus

The steady state axial transport of heat was the method used to study the mixing of solids. The experimental rigs were sim-

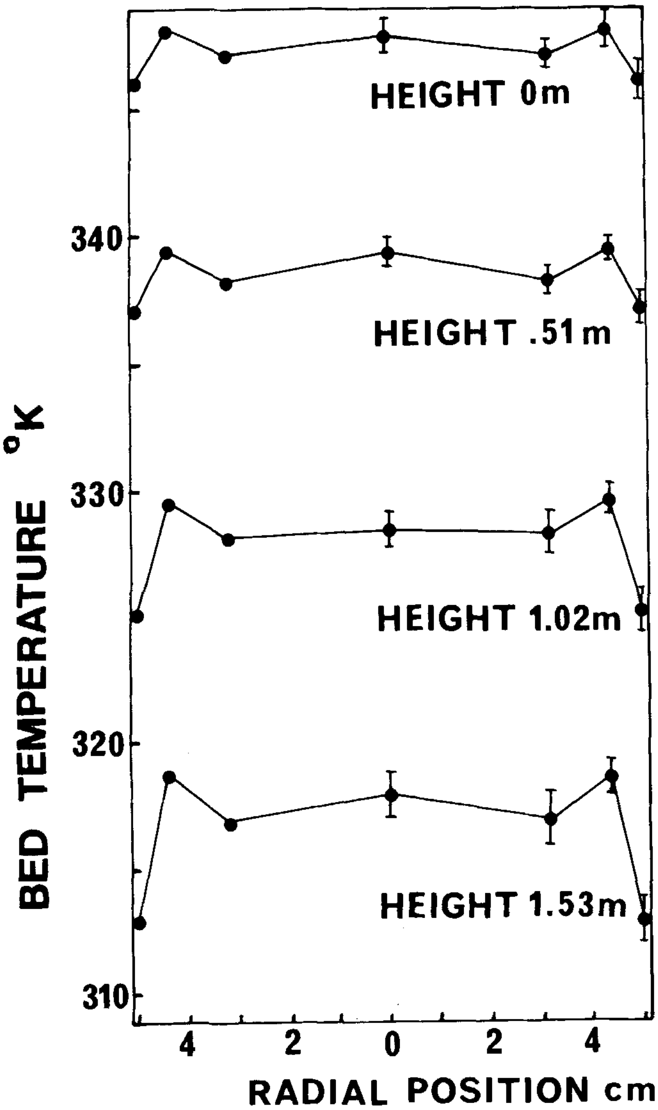

Fig. 4. Axial and radial temperature gradients in a 0.102 m diameter bed of FCC-Al at different heights in the experimental section (U-U_{mf} = 0.03 m/s).

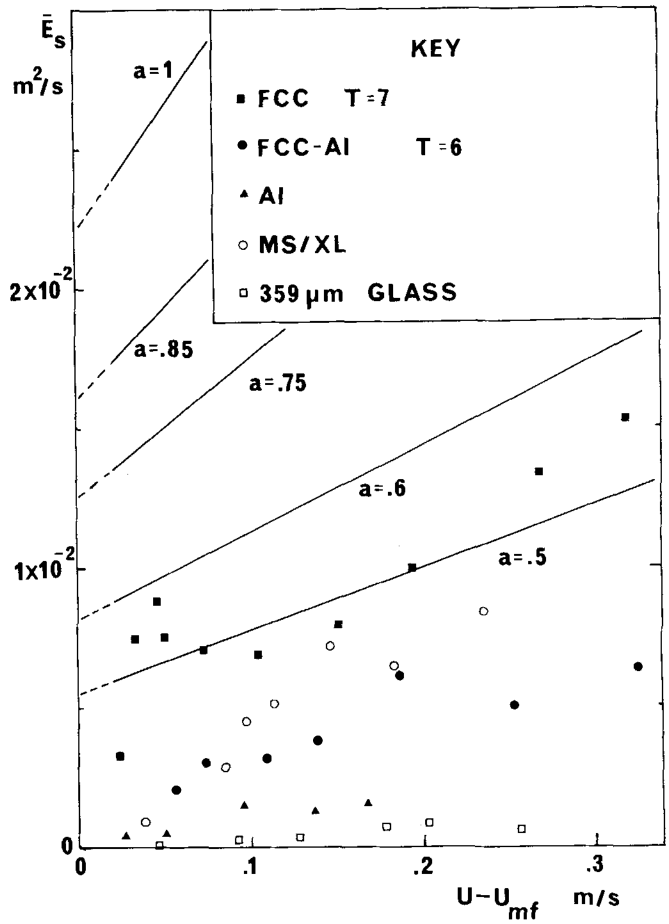

Fig. 5. Axial solids diffusivity $\underline{E_S}$ in 0.051 m diameter beds. Solid lines show Equation (28) with a value $T = 7$ for various values of the parameter a. Slug flow regimes, FCC round nosed slugs $T = 7$, FCC-Al round nosed slugs $T = 6$, Al wall and raining slugs, MS/XL round nosed and wall slugs, 359 μm glass raining slugs.

ilar to those used in earlier studies (Miyauchi et al., 1968; Shrikhande, 1955; Lewis et al., 1961-62). It was desired to investigate the axial mixing in smoothly slugging beds where the rate of slug coalescence was low. This resulted in beds of high aspect ratio. The lower ends of the tall, narrow beds were electrically heated and the upper ends cooled by water. Between these two sections, heat was transferred axially by the slugging bed through a heavily insulated adiabatic section (the experimental section).

Three different diameter beds were used, having circular cross sections and diameters of 0.051, 0.102, and 0.218 m. The basic design of the three beds was similar and is shown in Figure 3. Bed temperatures in the experimental section were measured by thermocouples located on a probe which passed down the axis of the equipment. The probe was located in position by guides and could be slid to any vertical height in the experimental section. The thermocouples on the probe were located at a number of radial positions to measure the bed temperature on the axis and close to the wall. Lewis et al. (1961-62), showed that radial temperature differences occurred close to the wall.

Above the cooling section, the cross-sectional area of the bed was greatly increased to form a solids disengaging section. Fine solids entrained in the exit gases were removed in a cyclone separator.

The two smaller diameter beds, 0.051 and 0.102 m, could be vibrated with an electromagnetic vibrator. A previous study showed that vibration aids the formation of smoothly slugging beds by reducing the tendency for solids to lock (Kehoe and Davidson, 1970).

The presence of gas slugs in the bed was detected by the change in electrical capacitance between two semicircular plates

Table 3. Physical Properties of Solids

Solid	Abbreviated name	U_{mf}, m/s	ρ_S, kg/m³	C_S, kJ/kg °K
Fluid cracking catalyst	FCC	1.8×10^{-3}	9.3×10^{-4}	6.7×10^{-1}
Fluid cracking catalyst-aluminium mixture	FCC-Al	2.5×10^{-3}	1.73×10^{-3}	8.8×10^{-1}
Aluminium powder	Al	6.2×10^{-3}	2.65×10^{-3}	9.6×10^{-1}
Glass microspheres	MS/XL	2.5×10^{-3}	2.45×10^{-3}	8.4×10^{-1}
Glass microspheres (closely sized)	395 μm glass	1.4×10^{-1}	2.45×10^{-3}	8.4×10^{-1}

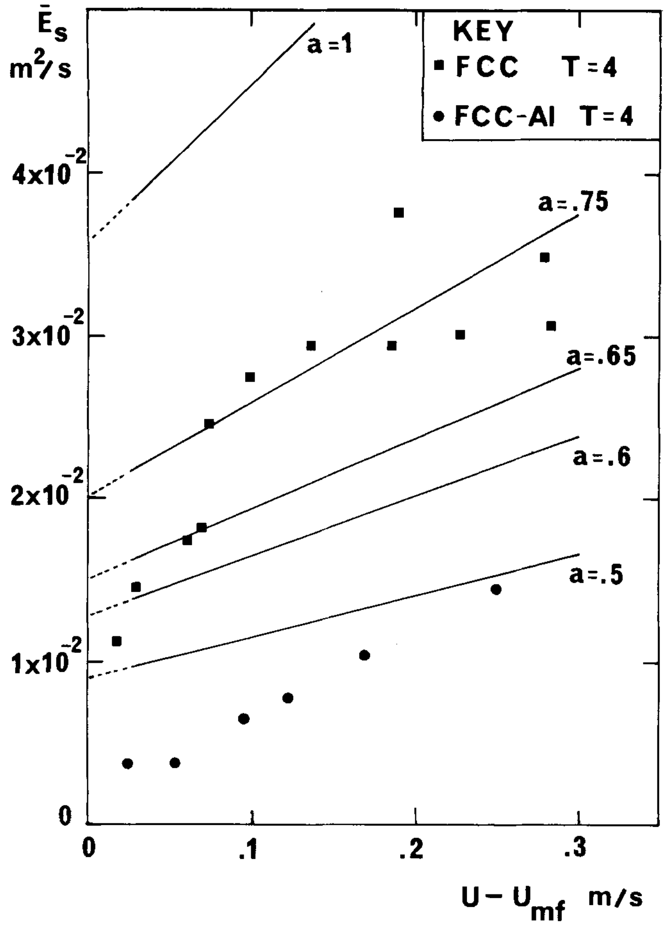

Fig. 6. Axial solids diffusivity $\bar{E}_S$ in 0.102 m diameter beds (smoothly slugging). Solid lines show Equation (28) with a value $T = 4$ for various values of the parameter a.

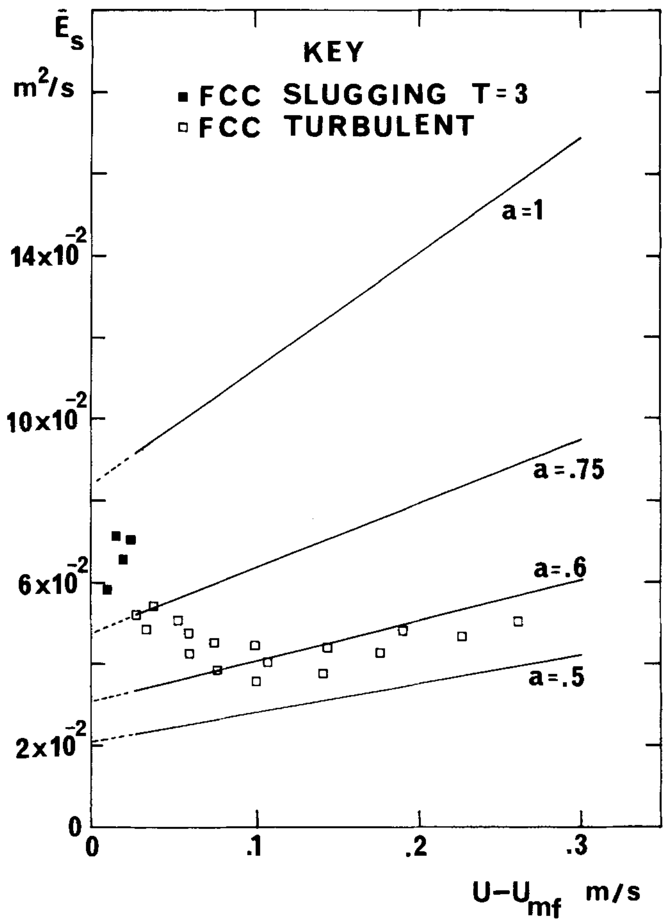

Fig. 7. Axial solids diffusivity $\bar{E}_S$ in a 0.218 m diameter bed of FCC. Solid lines show Equation (28) with a value of $T = 3$ for different values of the parameter a. The flow regimes are smoothly slugging for U-$U_{mf} < 0.025$ m/s and turbulent for greater air flow rates.

attached round the outside of the glass experimental section. The plates were attached to a proximity meter and an ultraviolet oscillograph which produced a visual record of the capacitance variations caused by the passage of gas slugs.

A number of different solids were used to form the smoothly slugging beds. The theoretical model shows that the axial thermal conductivity of the bed is dependent on the value of $\rho_S C_S$ for the solids [Equation (17)]. The solids used in this study were fluid cracking catalyst (FCC), a fluid cracking catalyst—aluminium powder mixture (FCC-Al), aluminium powder (Al), and two sizes of microspherical glass beads (MS/XL and 359 μ glass). The properties of the solids are given in Table 3 and by Thiel and Potter (1977). No segregation of the FCC-Al mixture was observed during the experimental work.

Experimental Method

The bed was simultaneously heated and cooled until steady state conditions were achieved. Bed temperatures were then recorded at different heights in the experimental section and at different radial positions. The cooling water flow rate and inlet and outlet water temperature were recorded to allow calculation of the quantity of heat being axially transferred through the experimental section by the slugging bed.

The bed was characterized by measuring the slug frequency, length, rise velocity, and interslug spacing. Values of these parameters are required to test the model for solids mixing.

The values of bed temperature measured by the thermocouples in the bed were analyzed statistically to calculate the axial temperature gradient in the experimental section. The best fit axial temperature gradient, at different radial positions, was computed by a least-squares linear regression of the bed temperatures. A value of the effective axial thermal conductivity could then be determined. Equation (9) was used to express this as an effective axial solids diffusivity for comparison with values predicted by the theoretical model.

DISCUSSIONS AND RESULTS

The slug flow regimes formed by different materials and values of slug frequency, length, rise velocity, and interslug spacing are reported elsewhere (Thiel, 1972; Thiel and Potter, 1977).

The effect of the axial thermocouple probe on the rise velocity of round nosed slugs was measured to ascertain whether the probe had any major effect on the slug dynamics. Slug rise velocities were measured with the thermocouple probe present and withdrawn from the experimental section. The presence of the probe made no significant difference to the slug rise velocities in beds of fluid cracking catalyst (FCC) (Thiel, 1972).

The mean axial temperature profiles in the experimental section were found to be linear. Radial temperature differences were confined to the region close to the bed wall. A typical result is shown in Figure 4. Vertical bars on the data points are the 95% confidence intervals for the mean bed temperature. Lewis, Gilliland, and Girouard (1961-62) obtained similar radial temperature differences and concluded that this was due to an overall circulation of solids in the bed.

Cracking Catalyst (FCC)—Round Nosed Slugs or Turbulent

This material formed round nosed slugs in the 0.051 and 0.102 m diameter beds, but in the 0.218 m bed, round nosed slugs only existed over a small velocity range. The turbulent breakdown (at $U - U_{mf} \geqq 0.025$ m/s) to smaller bubbles leads to a reduction in the axial mixing. The results are presented in Figures 5, 6, and 7. The model gives a reasonable prediction of the results

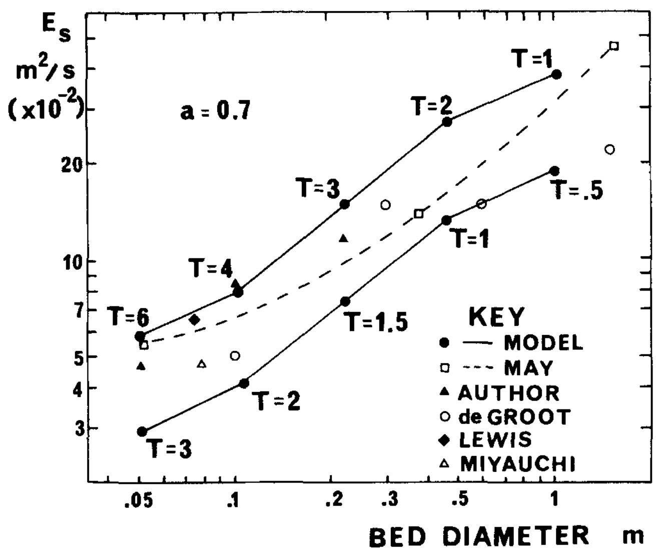

Fig. 8. Comparison of the model [Equation (28)] with all available experimental data, for probable values of interslug spacing T. The model is presented as a band which is bounded according to the expected range of T. Value of parameter $a = 0.7$.

with $a \simeq 0.5$ in the 0.051 m bed and $a \simeq 0.75$ in the 0.102 m bed. A value of $a = 0.5$ is consistent with the wake region occupying a volume of parabolic cross section, as shown in Figure 2. In the 0.218 m bed, the appropriate value is difficult to determine owing to the breakdown of round nosed slugs to the turbulent state. A value of $a \simeq 0.85$ fits the limited data obtained in beds in slug flow at low superficial gas velocities. In the turbulent state, a value of $a \simeq 0.6$ is appropriate.

Comparison of Model with Literature Data

A number of values of axial solids diffusivity measured in beds of fluid cracking catalyst and silica are available in the literature. Values of T measured simultaneously are not reported, but values may be inferred from Table 1 for similar diameter beds. Figure 8 shows all the available data for fluid cracking catalyst and the values of de Groot for silica plotted as E_S against bed diameter D, at a gas velocity $U - U_{mf} = 0.2$ m/s. The results predicted by the model [Equation (28)] are shown for values of T which represent the probable upper and lower values.

A value of the parameter $a = 0.7$ was used, although the value of a required in the model to fit the experimental results varied between 0.5 and 0.85. The results predicted by the model are seen to be in good general agreement with the values reported in the literature. It is noteworthy that the model predicts the scale effect of bed diameter with a fair degree of accuracy. Included on Figure 8 is May's curve for axial diffusivity of solids (May, 1959).

Squarenosed Slugs and Wall Slugs

When square nosed slugs exist (the raining bed), the axial dispersion coefficient is reduced markedly. In the cases where a mixture of wall slugs and raining bed slugs exist, there is also a reduction, though not so marked. Figure 5 shows axial mixing data for the 0.051 m bed, for different materials and different slugging regimes. Also plotted are the model predictions with different values of a. The dispersion coefficients for cracking catalyst and fine glass spheroids (MS/XL) are the highest values, while the lowest values measured are for coarse glass spheroids in which square nosed slugs predominated. The aluminium powder gave a mixture of wall (asymmetric), and raining slugs and intermediate values of the dispersion coefficient are obtained. These results are consistent with the different hydrodynamics of the round nosed and raining slug. As previously discussed, a wake exists behind a round nosed slug which causes an axial displacement of dense phase material. Such a gas slug would be expected to promote good axial mixing. In contrast, the raining slug will have a negligible wake, and thus the axial mixing would be expected to be lower. This result has been utilized in fluid bed reactors to improve the degree of chemical conversion Gelperin et al., (1970).

Anomalous Result

Figures 5 and 6 show an anomalous result in that the mixture of cracking catalyst and aluminium powder (FCC-Al), which formed round nosed slugs nevertheless yielded values of the dispersion coefficient only 40% of the corresponding values with cracking catalyst. The interslug spacing in beds of these two materials was similar; thus the model predicts equal axial solids diffusivities. No segregation of the FCC-Al mixture was observed during the experimental work. This anomaly has not been resolved. A possible explanation may lie in the assumption that solids are in thermal equilibrium. The very high rates of mixing which have been observed involve very rapid solids movement with little time for equilibration.

NOTATION

a = fraction of the interslug volume which is perfectly mixed
C = concentration
C_S = solids specific heat
D = bed diameter
D_e = equivalent sperical diameter of a bubble
D_S = axial solids diffusivity based on the cross-sectional area of dense phase in the bed
e = base of the natural logarithm
E_S = axial solids diffusivity based on the entire cross-sectional area
$\overline{E}_S$ = effective axial solids diffusivity, defined by Equation (9)
f = slug frequency
g = gravitational constant
j = cell number
J = constant defined by Equation (6)
L = length
L_S = length of a gas slug
t = time
T = dimensionless interslug spacing
u = superficial velocity
U = superficial gas velocity
U_{mf} = superficial gas velocity at incipient fluidization
U_{SA} = rise velocity of continuously generated slugs
U_{SD} = rise velocity of an isolated slug
v = volumetric flow rate
V = volume of a mixing cell

Greek Letters

ϵ_{mf} = voidage of an incipiently fluidized bed
ϵ_S = fraction of solids in the bed
ζ = length of a mixing cell
θ_j = temperature of the j^{th} mixing cell
θ_{jo} = temperature of the j^{th} mixing cell at time $t = 0$
$\theta_{j\tau}$ = temperature of the j^{th} mixing cell at time $t = \tau$
κ = effective thermal conductivity
ρ_S = solids density
τ = time constant defined by Equation (13)

LITERATURE CITED

Gelperin, N. I., V. G. Ainshtein, and L. I. Sukhanova, "Some Hydrodynamic Characteristics of Fluidization in the Piston Regime," *Theor. Found. Chem. Eng.*, **4**, 123 (1970).

de Groot, J. H., "Scaling Up of Fluidized Bed Reactors," *Proc. Intern. Symp. Fluidization*, p. 348, Netherlands Univ. Press, Eindhoven (1967).

Harrison, D., and L. S. Leung, "Coalescence of Bubbles in Fluidized Beds," *Symposium on the Interaction of Fluids and Particles*, p. 127, Inst. Chem. Engrs., London, England (1962).

Hovmand, S., and J. F. Davidson, "Chemical Conversion in a Slugging Fluidised Bed," *Trans. Inst. Chem. Engrs.*, **46**, T190 (1968).

——————, *in Fluidization*, J. F. Davidson and D. Harrison, ed., Chapt. 5, Academic Press, New York (1971).

Kehoe, P. W. K., and J. F. Davidson, "Continuously Slugging Fluidised Beds," *Chemeca '70*, Session 1, p. 97, Inst. Chem. Engrs., Butterworth's, England (1970).

Kunii, D., K. Yoshida, and O. Levenspiel, "Axial Movement of Solids in Bubbling Fluidised Beds," Tripartite Chem. Eng. Conf., Symposium on Fluidization 1, p. 72, Montreal, Canada (1968).

Levenspiel, O., in *Chemical Reaction Engineering*, Chapt. 9, Wiley, New York, (1962).

Lewis, W. K., E. R. Gilliland, and H. Girouard, "Heat Transfer and Solids Mixing in a Bed of Fluidised Solids," *Chem. Eng. Progr. Symposium Ser. No. 38, 58*, 87 (1961-62).

Matsen, J. M., and B. L. Tarmy, "Scale Up of Laboratory Fluid-Bed Data: the Significance of Slug Flow," *Chem. Eng. Progr. Symp. Ser. No. 101, 1*, 66 (1970).

May, W. G., "Fluidized-Bed Reactor Studies," *Chem. Eng. Progr.*, **55**, 49 (1959).

Miyauchi, T., H. Kaji, and K. Saito, "Fluid and Particle Dispersion in Fluid-Bed Reactors," *J. Chem. Eng. (Japan,)* **1**, 72 (1968).

Rowe, P. N., B. A. Partridge, A. G. Cheney, G. A. Henwood, and E. Lyall, "The Mechanisms of Solids Mixing in Fluidised Beds," *Trans. Inst. Chem. Engrs.*, *43*, T271 (1965).

Shrikhande, K. Y., "Apparent Thermal Conductivity of Batch Fluidised Solid Bed," *J. Sci. Ind. Res.*, **14B**, 457 (1955.)

Stewart, P. S. B., and J. F. Davidson, "Slug Flow in Fluidised Beds," *Powder Technol.*, **1**, 61 (1967).

Thiel, W. J., Ph.D. thesis, "Heat Transfer and Solids Mixing in Slugging Gas Fluidised Beds," Monash University, Australia (1972).

———, and O. E. Potter, "Slugging in Fluidized Beds," *Ind. Eng. Chem. Fundamentals*, **16**, 242 (1977).

Woollard, I. N. M., and O. E. Potter, "Solids Mixing in Fluidized Beds," *AIChE J.*, **14**, 338 (1968).

APPENDIX

Cell 1: $\theta_1 = 0$

Cell 2: $$v\rho_S C_S \epsilon_{mf}\theta_1 = v\rho_S C_S \epsilon_{mf}\theta_2 + V\rho_S C_S \epsilon_{mf}\left(\frac{d\theta_2}{dt}\right) \quad \text{(A1)}$$

$$\theta_1 = \theta_2 + \tau\frac{d\theta_2}{dt} \quad \text{(A2)}$$

At $t = 0$, $\theta_2 = \theta_{20}$, integrating Equation (A2), we get

$$\theta_2 = \theta_{20}\, e^{-t/\tau} \quad \text{(A3)}$$

Cell 3: the input to cell 3 is the output from cell 2:

$$\theta_2 = \theta_3 + \tau\left(\frac{d\theta_3}{dt}\right) \quad \text{(A4)}$$

Solving Equation (A4) by Laplace transforms, using Equation (A3) and at $t = 0$, $\theta_3 = \theta_{30}$ we get:

$$\theta_3 = \theta_{20}\left(\frac{t}{\tau}\right)e^{-t/\tau} + \theta_{30}e^{-t/\tau} \quad \text{(A5)}$$

For subsequent cells, the analysis continues in exactly the same way.

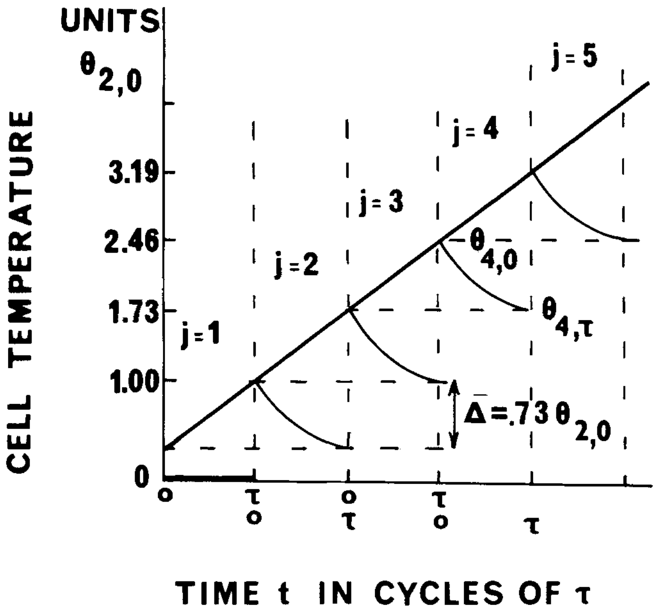

Fig. A1. Transient cell temperatures from the heat balance equations.

Cell 4: $$\theta_4 = \frac{\theta_{20}}{2!}\left(\frac{t}{\tau}\right)^2 e^{-t/\tau} + \theta_{30}\left(\frac{t}{\tau}\right)e^{-t/\tau} + \theta_{40}e^{-t/\tau} \quad \text{(A6)}$$

Cell 5: $$\theta_5 = \frac{\theta_{20}}{3!}\left(\frac{t}{\tau}\right)^3 e^{-t/\tau} + \frac{\theta_{30}}{2!}\left(\frac{t}{\tau}\right)^2 e^{-t/\tau} + \theta_{40}\left(\frac{t}{\tau}\right)e^{-t/\tau} + \theta_{50}e^{-t/\tau} \quad \text{(A7)}$$

Putting $t = \tau$ in Equations (A3), (A5), (A6), and (A7), indicating the temperature in cell j at time τ as $\theta_{j\tau}$, we get

$$\theta_{1\tau} = 0 \quad \text{(A8)}$$

$$\theta_{2\tau} = \theta_{20}e^{-1} \quad \text{(A9)}$$

$$\theta_{3\tau} = \theta_{30}e^{-1} + \theta_{20}e^{-1} \quad \text{(A10)}$$

$$\theta_{4\tau} = \theta_{40}e^{-1} + \theta_{30}e^{-1} + \theta_{20}(e^{-1}/2) \quad \text{(A11)}$$

$$\theta_{5\tau} = \theta_{50}e^{-1} + \theta_{40}e^{-1} + \theta_{30}(e^{-1}/2) + \theta_{20}(e^{-1}/6) \quad \text{(A12)}$$

At $t = \tau$, cell 1 is just empty, so cell 2 becomes cell 1 and in general cell j becomes cell $j - 1$. Therefore, the following relationships must hold:

$$\theta_{20} = \theta_{3\tau} \quad \text{(A13)}$$

$$\theta_{30} = \theta_{4\tau} \quad \text{(A14)}$$

$$\theta_{(j-1)0} = \theta_{j\tau} \quad \text{(A15)}$$

Using these relationships to solve Equations (A9) to (A12) we get

$$\theta_{20} = \theta_{20} \quad \text{(A16)}$$

$$\theta_{30} = 1.73\,\theta_{20} \quad \text{(A17)}$$

$$\theta_{40} = 2.46\,\theta_{20} \quad \text{(A18)}$$

$$\theta_{50} = 3.19\,\theta_{20} \quad \text{(A19)}$$

The average temperature difference between cells is equal to 0.73 θ_{20}. Figure A1 illustrates the transient cell temperatures predicted by the heat balance equations.

Manuscript received June 2, 1977; revision received November 21, and accepted December 7, 1977.